Pergamon

Chemical Engineering Science, Vol. 50, No. 4, pp. 631–640, 1995
Copyright © 1995 Elsevier Science Ltd
Printed in Great Britain. All rights reserved
0009–2509/95 $9.50 + 0.00

0009–2509(94)00440–4

EFFICIENT STIRRING IN PLANAR, TIME-PERIODIC LAMINAR FLOWS

F. RAYNAL and J. N. GENCE†
Laboratoire de Mécanique des Fluides et d'Acoustique, URA CNRS 263, Ecole Centrale de Lyon and Université Lyon I, 36 Avenue Guy de Collongue, 69131 Ecully Cédex, France

(*Received* 4 *July* 1993; *accepted in revised form* 2 *September* 1994)

Abstract—Laminar stirring in planar, time-periodic laminar flows is investigated, concentrating on the particular case of a cylindrical tank with two agitators. Using the Melnikov method, the choice of the kinematic parameters of the flow is discussed. A new parameter for stirring is defined, that takes into account both "spatial" and "temporal" efficiency.

1. INTRODUCTION

The two mechanisms that govern mixing are molecular diffusion and convection. However, under the sole action of molecular diffusion, a blob of dye spreads very slowly, showing that convection is essential to good mixing. The problem is how to set the fluid into motion in order to realize the most efficient mixing. In fact, making the flow turbulent is a good way to achieve mixing, but a random velocity flow-field is not essential, and even very simple laminar flows may exhibit some chaotic trajectories and hence reasonably efficient mixing, using less energy than required for turbulence.

Several examples of mixing in unsteady planar flows of inviscid fluid have been studied: Aref (1984) examined the case of two blinking vortices, and Khakhar *et al.* (1986) analyzed chaos in two model systems. Jones and Aref (1988) showed that even a very simple system without vorticity or rotation may achieve chaotic mixing. Rom-Kedar *et al.* (1990) made an analytical study of transport, mixing and chaos in an unsteady vortical flow.

The case of mixing in a Stokes flow between two eccentric cylinders has been considered, both experimentally and numerically (Aref and Balachandar, 1986; Swanson and Ottino, 1990); (Chaiken *et al.*, 1986, 1987). When the flow is three-dimensional, it need not be unsteady, since the third space coordinate z can play the role of time, for example in the partitioned-pipe mixer (Khakhar *et al.*, 1987) or in the twisted pipe (Jones *et al.*, 1989). The so-called A–B–C flow is another well-known three-dimensional steady flow that exhibits chaos (Dombre *et al.*, 1986).

In any flow configuration, the choice of parameters is crucial since chaos must be "global" (that is, it must cover the whole domain) for mixing to be truly efficient. Ottino (1989) showed the close connection between the notion of Lyapunov exponent from dynamical systems theory and the stretching of fluid elements. He also defined an "average efficiency", which is a normalized stretching rate. Rom-Kedar *et al.* (1990) have defined the new concept of "tangle dynamics" which allows them to compute the rate of transport of fluid between different regions of the flow. This method has been generalized to apply to planar time-periodic flows with arbitrary configurations (Rom-Kedar and Wiggins, 1990): these authors are able to determine in which part of the flow fluid particles should be chosen in order to undergo exponential stretching.

In this paper, we first discuss stirring in planar flows. Then we present a Stokes flow in a cylindrical tank, and propose an inviscid fluid flow having a similar topology of streamlines. Using analytical methods, we calculate the size of lobes for small perturbations. These lobes result from the intersections of a stable and an unstable manifold; we thus determine how this size depends globally on the parameters of the flow. Finally, we study different ways of "measuring" mixing, and define a new parameter of mixing which allows for both spatial and temporal aspects. We show that this parameter is a maximum when the period of the perturbation is of the same order as a characteristic time-scale of the unperturbed flow.

2. STIRRING IN PLANAR LAMINAR FLOWS: STRETCHING AND FOLDING

Stirring in planar chaotic flows is governed by mechanisms of stretching and folding. This fact is demonstrated rigorously by the presence of the well-known horseshoe maps in Poincaré sections of the flow (Ottino *et al.*, 1994). We do not want to introduce this concept here, but we will briefly explain how stretching and folding occur in planar flows from another point of view. Using this analysis we will derive a parameter for the "spatial" efficiency of mixing.

†Author to whom correspondence should be addressed.

A. *Lobe dynamics*

We consider a planar time-periodic flow. A Poincaré section P^{t_0} of that flow is classically defined as

$$P^{t_0}: \quad \mathbf{x}(t_0) \to \mathbf{x}(t_0 + T) \tag{2.1}$$

where T is the period of the flow. There is an infinity of such Poincaré maps, depending on the parameter t_0. In fact, they are all equivalent (Irwin, 1980), so that we will consider the Poincaré map $P \equiv P^0$:

$$P: \quad \mathbf{x}(0) \to \mathbf{x}(T). \tag{2.2}$$

Such a map possesses fixed points, that is, fluid particles of the flow that come back to the same location after one period T. It can be shown that these fixed points are either of elliptic or of hyperbolic type. The elliptic points are stable, whereas the hyperbolic points are unstable. Let $\mathbf{p}_0$ be a hyperbolic point; one can define the stable and unstable manifolds [resp. $W^s(\mathbf{p}_0)$ and $W^u(\mathbf{p}_0)$] associated to $\mathbf{p}_0$ as

$$W^s(\mathbf{p}_0) = \{\mathbf{x} \in \mathbb{R}^2, \lim_{n \to \infty} P^n(\mathbf{x}) = \mathbf{p}_0\} \tag{2.3}$$

$$W^u(\mathbf{p}_0) = \{\mathbf{x} \in \mathbb{R}^2, \lim_{n \to \infty} P^{-n}(\mathbf{x}) = \mathbf{p}_0\}. \tag{2.4}$$

These manifolds have some elementary properties:

(i) They are invariant under P.
(ii) Two stable (resp. unstable) manifolds cannot intersect.
(iii) A stable (resp. unstable) manifold cannot intersect itself.

For a discussion of all these definitions and properties, see for example Ottino (1989) or Wiggins (1990).

A.1. *Stretching*

The mechanism of stretching can be explained as associated with the intersection of a stable manifold $W^s(\mathbf{p}_1)$ and an unstable manifold $W^u(\mathbf{p}_0)$: Rom-Kedar *et al.* (1990) show that if two manifolds of different type intersect once, they do intersect infinitely many times, creating lobes. These lobes are denoted $E_{-1}, D_1, E_0, D_0, E_1, D_1$, etc. as shown in Fig. 1. These authors also prove that the image of a lobe E_i (resp. D_i) is the lobe E_{i+p}, $p \geqslant 1$ (resp. D_{i+p}). This mathematical property has a simple physical interpretation: the fluid which is in E_i at $t = 0$ is in E_{i+p} one period later, in E_{i+2p} at $t = 2T$, etc. Because of incompressibility, these lobes have the same area (they represent the same quantity of fluid). The fluid contained in a lobe thus represents the typical amount of fluid concerned in each period of the flow-field. Near the fixed point $\mathbf{p}_1$, the distance between two consecutive intersections become thinner and thinner, so that the lobes must become longer and longer in order to preserve area. This illustrates the mechanism of stretching of fluid elements, which is an essential process of stirring. Nevertheless, this is not enough: in order to achieve good stirring, the fluid elements have not only to be stretched but also to be folded. We will explain how this folding may happen in a simple geometry, where the stable and unstable manifolds result from the same hyperbolic point $\mathbf{p}_0$.

A.2. *Folding*

Let I be one of the intersection points of $W^u(\mathbf{p}_0)$ and $W^s(\mathbf{p}_0)$. We denote by $\mathscr{A}$ the region contained between the segments $[\mathbf{p}_0, I]$ of $W^u(\mathbf{p}_0)$ and $[I, \mathbf{p}_0]$ of $W^s(\mathbf{p}_0)$. Note in Fig. 2, we have chosen I so that $\mathscr{A}$ has a very simple shape. The lobes are denoted as before, see Fig. 2. The image of a lobe E_i is a lobe E_{i+p}. We will consider the case when $p = 1$. (The reasoning is not merely different when $p > 1$.) The image of E_1 is E_2, and, more generally, the image of the lobe E_n is the lobe E_{n+1}; all lobes E_i have the same area, and E_1 is in $\mathscr{A}$. Suppose that all the lobes E_i, $i \geqslant 1$, remained in $\mathscr{A}$; the area of $\mathscr{A}$ is finite, and there is an infinity of lobes E_i, $i \geqslant 1$, all having the same area. Thus some lobes E_i must intersect. However, this is impossible since it would mean that the unstable manifold $W^u(\mathbf{p}_0)$ intersects itself.

We have thus proved that the lobes E_i, $i \geqslant 1$, cannot all lie in $\mathscr{A}$. The only possibility for a given lobe E_m, $m \geqslant 1$, to escape from $\mathscr{A}$ is to intersect a lobe D_q, $q \geqslant 0$, since the unstable manifold cannot intersect itself. Thus $P^{-q}(E_m) = E_{m-q}$ intersects $P^{-q}(D_q) = D_0$. Let $m - q = r$. If $r = 1$, that is, if E_1 intersects D_0, the following argument can be applied to a subset $E_1^* \subset E_1$ such that $E_1^* \cap D_0 = \emptyset$. Thus we can restrict our attention to $r \neq 1$. For instance, we may consider the case when $r = 2$ (similar reasoning applies for $r \neq 2$). Thus suppose that E_2 intersects D_0. If we

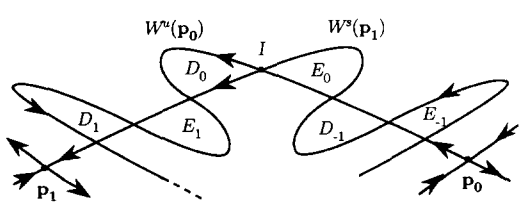

Fig. 1. Lobes created by the intersection of the manifolds $W^u(\mathbf{p}_0)$ and $W^s(\mathbf{p}_1)$.

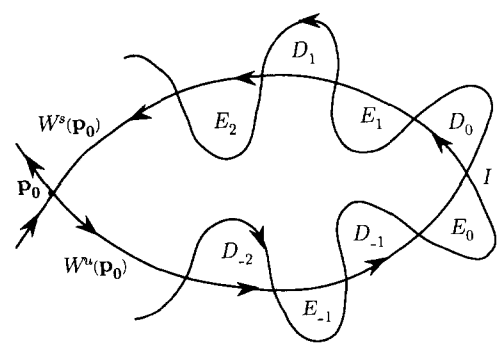

Fig. 2. Lobes created by the intersection of the manifolds $W^u(\mathbf{p}_0)$ and $W^s(\mathbf{p}_0)$.

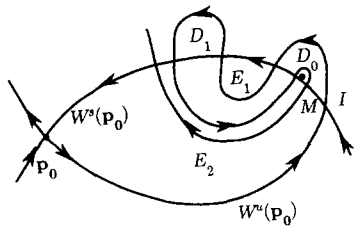

Fig. 3. Intersection of the lobe E_2 with the lobe D_0.

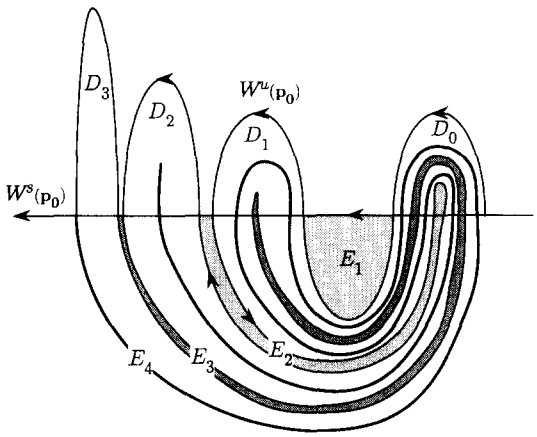

Fig. 4. Stretching and folding of the lobes $E_3, E_4, \ldots$.

consider a point M that belongs to the intersection (see Fig. 3), its image will be in $P(E_2) = E_3$, and also in $P(D_0) = D_1$. Thus E_3 intersects D_1. But E_3 can neither intersect E_2 nor E_1. It follows that E_3 will be as shown in Fig. 4. Similarly, E_4 must intersect D_2, without intersecting E_3, or E_2 and E_1.

Let us recast this argument in more physical language: the fluid that was in E_1 at $t = 0$ will be in E_2 at $t = T$, in E_3 at $t = 2T$, in E_4 at $t = 3T$, etc. If we compare the shapes of E_2 and E_3, we see that the fluid domain has been stretched and folded during one period of the flow-field. The conclusion is similar if the shape of E_3 is compared with that of $E_4 \ldots$. This behavior is in fact equivalent to the presence of horseshoe maps in the flow.

B. *Creation of a chaotic flow-field*

We have seen that if an intersection of manifolds occurs, then the flow is chaotic: the fluid is stretched and folded, and, after a while, the mechanism of molecular diffusion, even if initially weak, comes into play. The question of efficient stirring becomes how to create such an intersection of manifolds.

It is clear that the topology of the flow is crucial: chaos implies the existence of manifolds, associated with hyperbolic points of the Poincaré map. Let us consider a simple steady flow having a hyperbolic point $\mathbf{p}_0$. In such a stationary flow, satisfying an equation of the type

$$\dot{\mathbf{x}} = f(\mathbf{x}) \tag{2.5}$$

an unstable manifold either goes to infinity (of course, this may happen only when the domain is unbounded) or is also a stable manifold. In order to get chaotic trajectories, we add a periodic perturbation to this steady basic flow. The flow thus satisfies an equation of the type

$$\dot{\mathbf{x}} = f(\mathbf{x}) + \varepsilon g(\mathbf{x}, t) \tag{2.6}$$

where g is periodic in time, and f and g define a Hamiltonian flow-field (that is, a flow which satisfies $\operatorname{div} \mathbf{v} = 0$). It can be shown (Guckenheimer and Holmes, 1983) that for small ε, a Poincaré section P^{t_0} of this flow-field still possesses a hyperbolic point $\mathbf{p}_\varepsilon$ in an $O(\varepsilon)$-proximity of $\mathbf{p}_0$. Note that the case when the manifolds remain the same under the perturbation is still possible.

We will now apply these results to a practical example.

3. SPATIAL AND TEMPORAL EFFICIENCY OF STIRRING: A PRACTICAL EXAMPLE

A. *The Stokes flow*

We consider stirring in a cylindrical tank filled with very viscous fluid. Of course, the best way to achieve good mixing would be to make flow turbulent, but this would require high Reynolds numbers and a lot of energy since the fluid is very viscous. In order to create a laminar flow that is able to mix well, different principles must be followed: first of all, the steady basic flow must possess a hyperbolic point. As an example, we chose the case of two corotating cylinders. The rotation induces a circulation Γ of the velocity field around the surface of each cylinder, which appears as a basic parameter. We denote the distance between the center of the tank and a rotating cylinder by a, the radius of the tank by R, and the radius of each cylinder by r. We define a characteristic time-scale of the flow as the time T_1 it takes, when there is only one cylinder, for a fluid particle based at the origin to come back to its initial position, that is

$$T_1 = \frac{2\pi a}{\Gamma} 2\pi a = \frac{4\pi^2 a^2}{\Gamma}. \tag{3.1}$$

The Reynolds number Re_1 of the flow may be defined as

$$Re_1 = \frac{(\Gamma/2\pi a)2\pi a}{\nu} = \frac{\Gamma}{\nu} \ll 1 \tag{3.2}$$

where ν is the kinematic viscosity of the fluid. The streamlines of such a flow have been calculated numerically with a Reynolds number equal to 10^{-2} and are shown in Fig. 5 for the case $a = R/2$ and $r = R/10$. This flow clearly satisfies the requirement of a hyperbolic point. The second ingredient for efficient stirring is an unsteady, time-periodic flow superimposed on the basic flow. We have chosen a very simple perturbation: a sinusoidal contrarotating modulation of the rotation rate of the cylinders, as indicated in Fig. 6. Note that the perturbation must not have the same symmetries as the basic flow. For instance, if the

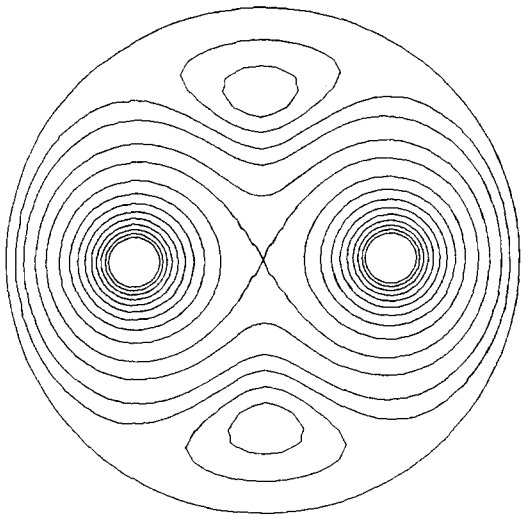

Fig. 5. Streamlines of the Stokes flow in a tank with two corotating cylinders.

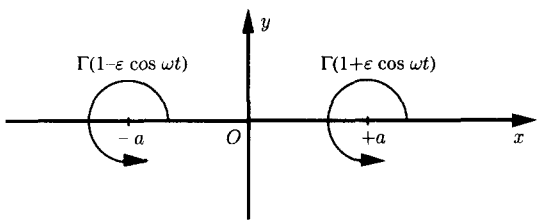

Fig. 6. Circulation of the velocity field at the surface of the cylinders.

perturbation were chosen to be a corotating modulation of the rotation of the cylinders, the trajectories would obviously remain on the curves shown in Fig. 5, which are not chaotic. A Reynolds number Re_2 based on the perturbation may be defined as

$$Re_2 = \frac{(2\pi a/T)2\pi a}{\nu} = \frac{4\pi^2 a^2}{T\nu} \ll 1 \qquad (3.3)$$

where $T = 2\pi/\omega$ is the period of the perturbation.

The parameters that define the flow are a, R, r, Γ, T and the relative strength of the perturbation ε. In this study we will not consider the influence of varying r and R, that is, the precise radius and position of the rotating cylinders in the tank. This is because we only want to describe trends, but obviously the cylinders must not be placed too near or too far from the center of the tank.

The independent dimensionless parameters based on a, Γ, T and ε are:

(i) ε (already dimensionless), the relative strength of the perturbation;
(ii) $\gamma = \Gamma T/\pi a^2$, the dimensionless period of perturbation.

Note that γ is not exactly the ratio at T and T_1, but this notation complies with that of Aref (1984) and Ottino (Khakhar *et al.*, 1986). If we computed the manifolds of the Poincaré section of the flow, we would see that the manifolds intersect when ε is nonzero, creating lobes. The size of the lobes, which is very important when deciding whether a given flow is able to mix well or not, will depend on the two parameters ε and γ.

The effect of varying ε is clear (the size of the lobes increases with the perturbation), but it appears that the dependence on γ is much less intuitive: is it better to perturb rapidly (T small, γ small), or on the contrary to perturb slowly (T large, γ large)? The only way to answer this is to compute the manifolds for a given value of ε and several values of γ, and measure the size of the lobes in each case. This means that a fine mesh of the domain should be used, and that the Navier–Stokes equations must be solved in the Stokes approximation at each time-step (of course the time-step must be small enough compared to the characteristic time-scales of the flow). The manifolds must then be tracked, which is a delicate task in itself (Franjione and Ottino, 1987). Of course these operations must be repeated for each value of γ (except for the mesh generation of course). In short, this is almost impossible if the flow-field is not known analytically, and of course no analytical solution—even approximate—exists for this flow. In fact, we do not need an exact solution of our problem; we do not mind whether the flow-field is correct in detail or not, but we do need some global information: how does stirring depend globally on the parameter γ?

B. *A similar problem in an inviscid fluid*

Let us consider the case of two parallel line vortices in nonviscous fluid placed respectively at $A(-a, 0)$ and $B(a, 0)$, with circulations reflecting those of the cylinders in Fig. 6. For simplicity, we neglect the influence of a/R and we suppose that the fluid domain is infinite. The streamlines of the basic flow (that is, when ε is zero) are shown in Fig. 7. Their topology is exactly the same as in the above Stokes flow, except for the absence of the recirculation zones that were due to the boundaries. Note that the flow-field itself will not be very different, at least in the neighborhood of each cylinder where the influence of the other is weak, since velocity decays like $1/r$ when moving away from a cylinder in a Stokes flow, just as for the vortex line in an inviscid fluid. Moreover, the Stokes problem has exactly the same symmetries as the above inviscid problem; hence all results based on properties of symmetry carry across to a real Stokes flow.

B.1. *Equations of motion*

The global flow-field (basic flow plus perturbation) has the stream function ψ which is given by

$$\psi = -\frac{\Gamma(1-\varepsilon\cos\omega t)}{4\pi}\ln \mathrm{AM}^2 - \frac{\Gamma(1+\varepsilon\cos\omega t)}{4\pi}\ln \mathrm{BM}^2 \qquad (3.4)$$

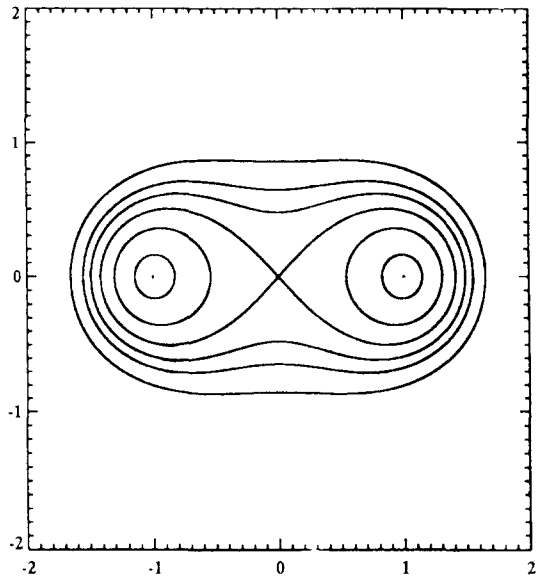

Fig. 7. Streamlines of the inviscid fluid flow with two corotating vortex-lines.

with

$$\mathrm{AM}^2 = (x + a)^2 + y^2, \quad \mathrm{BM}^2 = (x - a)^2 + y^2.$$

Thus we can obtain the equations of motion of the fluid particles:

$$\begin{aligned} \frac{\mathrm{d}x}{\mathrm{d}t} &= -\frac{\Gamma}{\pi} y \frac{x^2 + y^2 + a^2}{d^4} - \frac{\Gamma}{\pi} \varepsilon \cos \omega t \, a \frac{2xy}{d^4} \\ \frac{\mathrm{d}y}{\mathrm{d}t} &= +\frac{\Gamma}{\pi} x \frac{x^2 + y^2 - a^2}{d^4} \\ &\quad + \frac{\Gamma}{\pi} \varepsilon \cos \omega t \, a \frac{x^2 - y^2 - a^2}{d^4} \end{aligned} \tag{3.5}$$

where d is defined as $d^4 = \mathrm{AM}^2 \, \mathrm{BM}^2$.

In order to make the equation dimensionless, we introduce the parameter γ defined previously, and we take a as length-scale and T as time-scale. We let $c = d/a$. Thus we obtain

$$\begin{aligned} \frac{\mathrm{d}x}{\mathrm{d}t} &= -\gamma y \frac{x^2 + y^2 + 1}{c^4} - \gamma \varepsilon \cos 2\pi t \frac{2xy}{c^4} \\ \frac{\mathrm{d}y}{\mathrm{d}t} &= +\gamma x \frac{x^2 + y^2 - 1}{c^4} + \gamma \varepsilon \cos 2\pi t \frac{x^2 - y^2 - 1}{c^4} \end{aligned} \tag{3.6}$$

with

$$\begin{aligned} c^4 &= [(x - 1)^2 + y^2][(x + 1)^2 + y^2] = (x^2 + y^2)^2 \\ &\quad + 2(y^2 - x^2) + 1. \end{aligned} \tag{3.7}$$

B.2. *Choice of the Poincaré section*

As already explained, there is an infinity of Poincaré maps P^{t_0} depending on the parameter t_0 and we choose the Poincaré map P^0 since this choice has no influence on the size of the lobes (area preservation).

C. *The Melnikov method*

There are two possibilities when the manifolds are submitted to an area-preserving perturbation: either they remain the same, or they intersect at an infinity of points. In order to prove rigorously that the manifolds really intersect, we must use a standard analytical tool of small perturbations theory called the Melnikov method.

This technique applies to flow-fields of the type

$$\dot{\mathbf{x}} = f(\mathbf{x}) + \varepsilon g(\mathbf{x}, t) + O(\varepsilon^2) \tag{3.8}$$

where f and g are two functions defined on $\mathbb{R}^2$, g is periodic in time, and f defines a Hamiltonian flow-field. In our case, g also defines a Hamiltonian flow-field; moreover our model does not contain terms of $O(\varepsilon^2)$. The Melnikov method was developed by Melnikov in 1963. It predicts the behavior of the manifolds by calculating, at order ε, the algebraic distance $d(t_0)$ between the two manifolds of the Poincaré map P^{t_0} at a given point $\mathbf{q}_0(0)$ on the unperturbed manifold. $\mathbf{q}_0(t)$ is the unperturbed manifold, that is, the manifold corresponding to $\varepsilon = 0$. We define $\mathbf{q}_\varepsilon^u(t_0)$ and $\mathbf{q}_\varepsilon^s(t_0)$ as the unique points of P^{t_0} on $W^u(\mathbf{p}_\varepsilon)$ and $W^s(\mathbf{p}_\varepsilon)$ "closest" to $\mathbf{p}_\varepsilon$ and lying on

$$f^\perp[\mathbf{q}_0(0)] = \{ -f_y[\mathbf{q}_0(0)], f_x[\mathbf{q}_0(0)] \} \tag{3.9}$$

the normal to $f[\mathbf{q}_0(0)]$ at $\mathbf{q}_0(0)$, see Fig. 8. As usual, $d(t_0)$ is defined as

$$d(t_0) = \frac{f^\perp[\mathbf{q}_0(0)]}{\| f^\perp[\mathbf{q}_0(0)] \|} \cdot [\mathbf{q}_\varepsilon^u(t_0) - \mathbf{q}_\varepsilon^s(t_0)]. \tag{3.10}$$

Note that in Fig. 8, $d(t_0)$ is positive. Melnikov's theory now says that, for small ε, this distance can be calculated at order ε without any knowledge of $\mathbf{q}_\varepsilon^u(t_0)$ or $\mathbf{q}_\varepsilon^s(t_0)$. $d(t_0)$ is simply given by [see Guckenheimer and Holmes (1983, Chap. 4)]

$$d(t_0) = \varepsilon \frac{M(t_0)}{|f[\mathbf{q}_0(0)]|} + O(\varepsilon^2) \tag{3.11}$$

with

$$M(t_0) = \int_{-\infty}^{+\infty} f[\mathbf{q}_0(t - t_0)] \wedge g[\mathbf{q}_0(t - t_0), t] \, \mathrm{d}t: \quad \text{the Melnikov function.} \tag{3.12}$$

Here the wedge product is defined by $\mathbf{a} \wedge \mathbf{b} = a_x b_y - a_y b_x$.

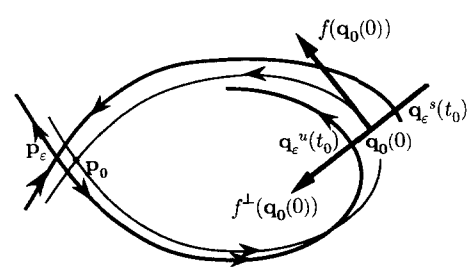

Fig. 8. Definition of the distance between two manifolds $|d(t_0)| = \| \mathbf{q}_\varepsilon^u(t_0) - \mathbf{q}_\varepsilon^s(t_0) \|$.

We next need to introduce a parametrization of the unperturbed manifolds that defines the point $\mathbf{q}_0(0)$ where the distance $d(t_0)$ is calculated [since this point $\mathbf{q}_0(0)$ can be chosen anywhere on the two unperturbed manifolds]. Suppose that $\mathbf{q}_0(0)$ lies on the right manifold, as in Fig. 9. We may then parametrize it by the time t_1 it takes to come from J on the unperturbed manifold $\mathbf{q}_0(t)$. Thus J is defined as $\mathbf{q}_0(-t_1)$ since $\mathbf{q}_0(-t_1+t_1)$ is $\mathbf{q}_0(0)$. In Fig. 9, t_1 is positive. Similarly, if $\mathbf{q}_0(0)$ lies on the left unperturbed manifold, we parametrize it by the time t_1 it takes to come from J'; we denote the distance between the two manifolds at the point $\mathbf{q}_0(0)$ by $d_{t_1}(t_0)$. We can now introduce the parameter t_1 into the Melnikov function:

$$\begin{aligned} M_{t_1}(t_0) &= \int_{-\infty}^{+\infty} f[\mathbf{q}_0(t-t_0+t_1-t_1)] \\ &\quad \wedge\, g[\mathbf{q}_0(t-t_0+t_1-t_1), t]\,\mathrm{d}t \\ &= \int_{-\infty}^{+\infty} f[\mathbf{q}_0(t-t_1)] \wedge g[\mathbf{q}_0(t-t_1), t \\ &\quad + t_0 - t_1]\,\mathrm{d}t. \end{aligned} \tag{3.13}$$

If we let $t_0 = 0$ (Poincaré map P^0) we have

$$M_{t_1}(0) = \int_{-\infty}^{+\infty} f[\mathbf{q}_0(t-t_1)] \wedge g[\mathbf{q}_0(t-t_1), t-t_1]\,\mathrm{d}t. \tag{3.14}$$

In the case of our flow-field, considerations of symmetry lead us to a simple expression for the Melnikov function (see the calculation in the Appendix):

$$M_{t_1}(0) = F(\gamma)\sin 2\pi t_1 \quad \text{with} \quad F(\gamma) = \pm\,\gamma\,\frac{\sinh(\pi^2/2\gamma)}{\cosh(\pi^2/\gamma)} \tag{3.15}$$

where the sign $+$ denotes the case when the point $\mathbf{q}_0(0)$ lies on the right unperturbed manifold, as in Fig. 9, and the sign $-$ is to be taken when $\mathbf{q}_0(0)$ lies on the left manifold.

D. *Size of the lobes*

When ε is equal to zero, the manifolds are the same and the size of the lobes is zero, When ε is nonzero, one can expand the size of the lobes $S(\varepsilon)$ as a series in ε:

$$S(\varepsilon) = \varepsilon S_1(\gamma) + \varepsilon^2 S_2(\gamma) + \varepsilon^3 S_3(\gamma) + \cdots \tag{3.16}$$

so that, for small ε, $S(\varepsilon)$ may be approximated by

$$S(\varepsilon) \approx \varepsilon S_1(\gamma) + O(\varepsilon^2). \tag{3.17}$$

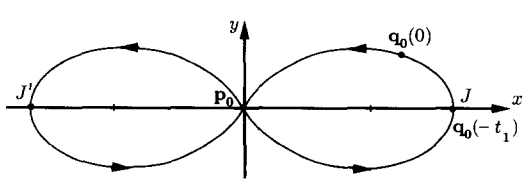

Fig. 9. Parametrization of the unperturbed manifolds.

Note that, because the equations are written in dimensionless form, all the quantities that are defined hereafter are dimensionless too. In particular the surface area S is dimensionless and the corresponding dimensional value σ is given by

$$\sigma = a^2 S = \varepsilon\sigma_1 + \varepsilon^2\sigma_2 + \cdots \tag{3.18}$$

A direct application of the Melnikov function allows the calculation of the surface of the lobes at order ε (Rom-Kedar *et al.*, 1990), namely $\varepsilon S_1(\gamma)$, as follows. As we have already explained, we consider the Poincaré map P^0 ($t_0 = 0$), and we denote the curvilinear abscissa along the unperturbed manifold by $s(t_1)$: $s(t_1)$ is the curvilinear distance between J (or J') and $\mathbf{q}_0(0)$. In Fig. 9, $s(t_1)$ is positive; moreover, $\mathrm{d}s/\mathrm{d}t_1$ is positive. Let t_{1_1} and t_{1_2} be two consecutive zeros of $M_{t_1}(0)$. The dimensionless surface of a lobe, denoted $S(\varepsilon)$, is thus

$$\begin{aligned} S(\varepsilon) &= \left| \int_{s(t_{1_1})}^{s(t_{1_2})} d_{t_1}(0)\,\mathrm{d}s \right| \\ &= \varepsilon \left| \int_{t_{1_1}}^{t_{1_2}} \frac{M_{t_1}(0)}{\|f[\mathbf{q}_0(0)]\|}\,\frac{\mathrm{d}s}{\mathrm{d}t_1}\,\mathrm{d}t_1 \right| + O(\varepsilon^2) \end{aligned} \tag{3.19}$$

where $\mathrm{d}s/\mathrm{d}t_1$ is the norm of the velocity on the unperturbed manifold at $s(t_1)$, namely $\|f[\mathbf{q}_0(0)]\|$. This remark leads to a very simple analytical expression for $S(\varepsilon)$ at order ε:

$$S(\varepsilon) = \varepsilon \left| \int_{t_{1_1}}^{t_{1_2}} M_{t_1}(0)\,\mathrm{d}t_1 \right| + O(\varepsilon^2). \tag{3.20}$$

In our model, the expression for $M_{t_1}(0)$, integrated between $t_{1_1} = 0$ and $t_{1_2} = 1/2$, leads to

$$S(\varepsilon) = \frac{\sigma(\varepsilon)}{a^2} = \varepsilon\,\frac{|F(\gamma)|}{\pi} + O(\varepsilon^2) \tag{3.21}$$

so that

$$S_1(\gamma) = \frac{|F(\gamma)|}{\pi} \tag{3.22}$$

where S_1 is a monotonous function, which is shown in Fig. 10. Moreover,

$$S_1(\gamma) \underset{\gamma\to\infty}{\sim} \frac{\gamma}{\pi}\,\frac{\pi^2}{2\gamma} = \frac{\pi}{2} \tag{3.23}$$

$$S_1(\gamma) \underset{\gamma\to 0}{\sim} \frac{\gamma}{\pi}\,e^{-\pi^2/2\gamma} \underset{\gamma\to 0}{\rightarrow} 0. \tag{3.24}$$

The maximum size of the lobes is thus

$$S_{\max} = \varepsilon\,\frac{\pi}{2} + O(\varepsilon^2). \tag{3.25}$$

E. *Different ways to "measure" mixing*

When talking about chaos, the natural parameter is the Lyapunov exponent, whose definition is based on the fact that a linear fluid element in a chaotic flow-field will experience exponential stretching: if $\delta\mathbf{m}(0)$ is a fluid material element, whose length is small enough, and if $\delta\mathbf{m}(nT)$, n being large, is the same fluid

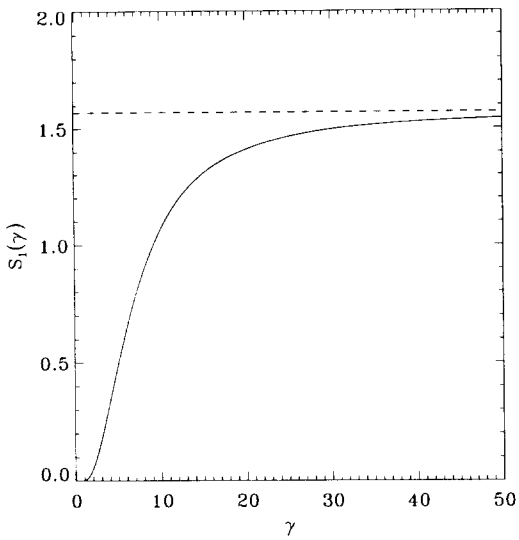

Fig. 10. Graph of $S_1(\gamma)$.

element after n periods of the flow-field, then we have

$$\|\delta\mathbf{m}(nT)\| \approx \|\delta\mathbf{m}(0)\| e^{\alpha n T} \tag{3.26}$$

where α is called the "Lyapunov exponent". α is a local parameter, since it depends on the position and orientation of $\delta\mathbf{m}(0)$. However, chaos must be global — that is, it must cover the whole fluid domain — for stirring to be truly efficient. Hence we propose to use the size of the lobes as a parameter for measuring stirring, since it represents the typical amount of fluid convected at each period with chaotic trajectories: this size grows with ε and γ, which is physically reasonable.

Now let us return to the physical meaning of the dimensionless parameter γ: it was defined as the ratio of the period of perturbation T to a typical time-scale of the basic flow. There are two possibilities for increasing γ: either the typical time of the basic flow is decreased, which implies that Γ is increased [however, this possibility is limited by the inequality (3.2)], or else T is made larger, which is allowed by eq. (3.3). But if the period T is very long, then mixing will also take a long time, so that even if stirring is "spatially" efficient, it is not "temporally" efficient. Thus we propose a more "practical" parameter to describe mixing, μ, which is defined as

$$\mu = \frac{\sigma}{T} \tag{3.27}$$

that is, the size of the typical dimensional chaotic surface convected per unit time. In dimensionless terms, we consider the parameter m:

$$m = \frac{S}{T/(\pi\alpha^2/\Gamma)} = \frac{S}{\gamma} \tag{3.28}$$

where S is the dimensionless area of the lobes, and where the period of the perturbation T has been made dimensionless through γ, as before.

For small ε, using eq. (3.21), m may be expressed as

$$m = \varepsilon \frac{\sinh(\pi^2/2\gamma)}{\cosh(\pi^2/\gamma)} + O(\varepsilon^2) = \varepsilon m_1 + O(\varepsilon^2). \tag{3.29}$$

The quantity m_1 varies with γ as shown in Fig. 11; the maximum is reached for

$$\gamma = \frac{\pi^2}{2\ln(1+\sqrt{3})/\sqrt{2}} \simeq 7.5. \tag{3.30}$$

As already noted, γ is not the ratio of T and T_1: let us therefore define $\gamma' = T/T_1$, so that

$$\gamma' = \frac{T}{T_1} = \frac{\Gamma T}{4\pi^2 a^2} = \frac{\gamma}{4\pi}. \tag{3.31}$$

The maximum of m_1 is reached when

$$\gamma' = \frac{7.5}{4\pi} \simeq 0.6 \tag{3.32}$$

that is, *when the period of perturbation is roughly of the same order of magnitude as the time-scale of the basic flow.*

The above result has been derived analytically using perturbation theory and it is of interest to compare it with numerical results for moderate ε (not small). Figure 12(a)–(c) shows three computed Poincaré maps with $\varepsilon = 1$ (moderately large perturbations) for three values of γ. It can be seen that a good stirring process occurs for $\gamma = 10$, that is, for $\gamma' = T/T_1 = 0.8$, i.e. $T \simeq T_1$. When $\gamma = 15$, a nonchaotic zone reappears around the left vortex, and persists when γ is further increased. This phenomenon appears in all chaotic two-dimensional flow-fields previously studied when the perturbation parameter is increased sufficiently (Aref, 1984; Jones and Aref, 1988); it may be explained as a "relaminarization" process, similar to what is observed in one dimension in the interval

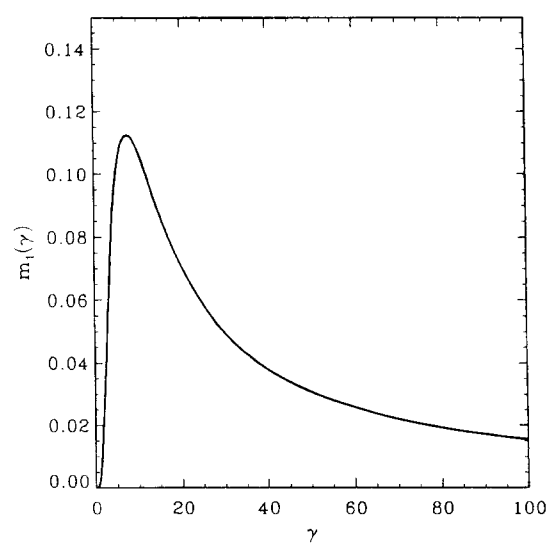

Fig. 11. Graph of $m_1(\gamma)$.

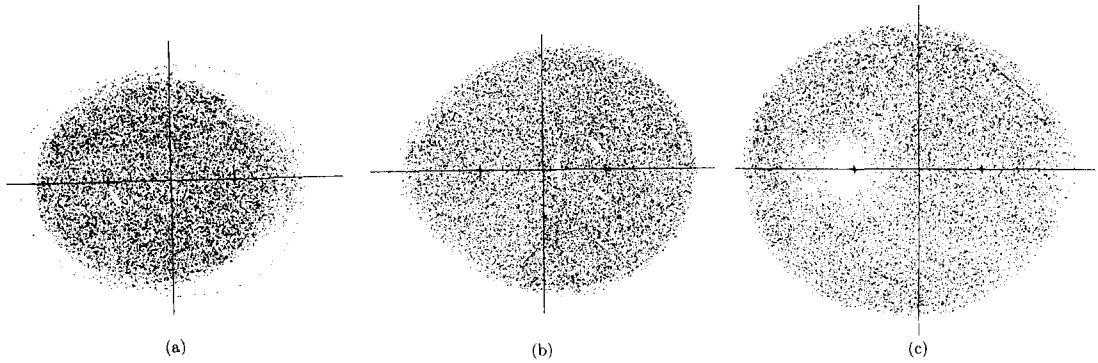

Fig. 12. Three Poincaré sections $\varepsilon = 1$: (a) $\gamma = 7.5$; (b) $\gamma = 10$; (c) $\gamma = 15$.

$[0, 1]$ with a function f_λ defined as

$$f_\lambda(x) = \lambda x(1 - x), \quad 0 \leqslant \lambda \leqslant 4 \tag{3.33}$$

when λ varies from 0 to 4 (Bergé *et al.*, 1984).

Let us sum up: the period of the flow-field must not be chosen too small, because then chaos is not global. Neither must it be too large, because on the one hand stirring is no longer temporally efficient, and on the other hand some elliptic zones may appear. In this example of inviscid flow, it has been found both *analytically and numerically* that the best stirring efficiency is reached when the period of the flow-field is of the same order of magnitude as a characteristic time-scale of the basic flow.

However, when coming back to the concrete problem of a Stokes flow in a cylindrical tank, one can wonder whether this maximum of $m(\gamma)$ will still exist. Consider the dimensional parameter

$$\mu = \frac{\sigma}{T}. \tag{3.34}$$

For a given value of Γ, we consider the asymptotic limits when T goes to zero and infinity, in order to show the existence of a maximum in the general case. This poses the problem of the existence of μ for $T = 0$. Of course, one expects that $\sigma(T = 0) = 0$, which means physically that when perturbed too quickly ($\omega = 2\pi/T \to \infty$), a system cannot "keep up with" the perturbation, and therefore does not even feel it. In our case of two vortices in inviscid fluid, the equivalent of $\sigma_1(T)$ for small T is

$$\sigma_1(T) = a^2 S_1\left(\frac{\Gamma T}{\pi a^2}\right) \underset{T \to 0}{\sim} a^2 \frac{\gamma}{\pi} e^{-\pi^2/2\gamma} = \frac{\Gamma T}{\pi^2} e^{-\pi^3 a^2/2\Gamma T} \tag{3.35}$$

so that $\sigma_1(T)$ is exponentially small when T tends to zero. In fact, this constitutes a universal result (Zaslavsky *et al.*, 1991): when perturbed at high frequency ($\omega = 2\pi/T \gg 1$), the width of the stochastic layer (that is to say the region where the chaos takes place) appearing around the manifold is exponentially small, even for large perturbations, which implies that

$$\mu(T = 0) = 0. \tag{3.36}$$

In the opposite limit when T tends to infinity, the surface area of lobes, even if increasing with T, of course remains smaller than the size of the tank, πR^2 in the case of a cylindrical tank of radius R, and, whatever the strength of the perturbation, we have

$$\mu(T) = \frac{\sigma(T)}{T} \leqslant \frac{\pi R^2}{T} \xrightarrow[T \to \infty]{} 0. \tag{3.37}$$

This means that $\mu(T)$ will have a maximum in any closed system, whatever the strength of the perturbation, and this result is clearly of importance in the design of two-dimensional time-periodic mixing apparatuses.

4. SUMMARY AND CONCLUSION

In this paper, we have explained how the mechanisms of stretching and folding can be related to the dynamics of lobes. We have focused on the particular problem of mixing in a cylindrical tank with two corotating cylinders with a sinusoidal contrarotating modulation. Our aim has not been to solve the problem exactly, but to bring out some of its general mixing properties; to this end we have studied a flow of an inviscid fluid having streamline topology similar to that of the Stokes flow. We have calculated the size of the lobes analytically for small perturbations, and found that the period of perturbation must be large enough for stirring to be spatially efficient. In order to have temporal efficiency as well, we have introduced a "practical" efficiency parameter defined as the ratio of the surface area of the lobes to the period of the perturbation. It was found analytically that, for small perturbation, this parameter is zero when T is small or large, and has an intermediate maximum when the period of perturbation is of the same order of magnitude as a characteristic time-scale of the flow. Furthermore, this order of magnitude has been numerically shown to remain relevant for large perturbations. This result may be of importance when creating a chaotic flow-field: the characteristic time-scales must be chosen to be of the same order of magnitude so that time is not wasted on trial and error experiments which will be fruitless.

Acknowledgements—We wish to thank J. F. Scott for helpful discussions.

REFERENCES

Aref, H., 1984, Stirring by chaotic advection. *J. Fluid Mech.* **143**, 1–21.

Aref, H. and Balachandar, S., 1986, Chaotic advection in a Stokes flow. *Phys. Fluids* **29**, 3515–3521.

Bergé, P., Pomeau, Y. and Vidal, C., 1984, *L'ordre dans le Chaos*. Hermann, Paris.

Chaiken, J., Chevray, R., Tabor, M. and Tan, Q. M., 1986, Experimental study of Lagrangian turbulence in Stokes flow. *Proc. R. Soc. London A* **408**, 105.

Chaiken, J., Chu, C. K., Tabor, M. and Tan, Q. M., 1987, Lagrangian turbulence and spatial complexity in a Stokes flow. *Phys. Fluids* **30**, 687–694.

Dombre, T., Frisch, U., Greene, J. M., Henon, M., Mehr, A. and Soward, A. M., 1986, Chaotic streamlines in the ABC flows. *J. Fluid Mech.* **167**, 353–391.

Franjione, J. G. and Ottino, J. M., 1987, Feasibility of numerical tracking of material lines and surfaces in chaotic flows. *Phys. Fluids* **30**, 3641.

Gradshteyn, I. S. and Ryzhik, I. M., 1980, *Tables of Integrals, Series and Products* (corrected and enlarged edition). Academic Press, New York.

Guckenheimer, J. and Holmes, P., 1983, *Non-linear Oscillations, Dynamical Systems, and Bifurcation of Vector Fields*. Springer, Berlin.

Irwin, M. C., 1980, *Smooth Dynamical Systems*. Academic Press, New York.

Jones, S. W. and Aref, H., 1988, Chaotic advection in pulsed source-sink systems. *Phys. Fluids* **31**, 469–485.

Jones, S. W., Thomas, O. M. and Aref, H., 1989, Chaotic advection by laminar flow in a twisted pipe. *J. Fluid Mech.* **209**, 335–357.

Khakhar, D. V., Franjione, J. G. and Ottino, J. M., 1987, A case study of chaotic mixing in deterministic flows: the partitioned pipe mixer. *Chem. Engng Sci.* **42**, 2909–2926.

Khakhar, D. V., Rising, H. and Ottino, J. M., 1986, Analysis of chaotic mixing in two model systems. *J. Fluid Mech.* **172**, 419–451.

Ottino, J. M., 1989, *The Kinematics of Mixing: Stretching, Chaos, and Transport*. Cambridge University Press, Cambridge.

Ottino, J. M., Jana, S. C. and Chakravarthy, V. S., 1994, From Reynolds stretching and folding to mixing studies using horseshoe maps. *Phys. Fluids* **6**, 685–699.

Rom-Kedar, V., Leonard, A. and Wiggins, S., 1990, An analytical study of transport, mixing and chaos in an unsteady vortical flow. *J. Fluid Mech.* **214**, 347–394.

Rom-Kedar, V. and Wiggins, S., 1990, Transport in two-dimensional maps. *Arch. Ration. Mech. Anal.* **109**, 239–298.

Swanson, P. D. and Ottino, J. M., 1990, A comparative computational and experimental study of chaotic mixing in viscous fluids. *J. Fluid Mech.* **213**, 227–249.

Wiggins, S., 1988, *Global Bifurcations and Chaos — Analytical Methods*. Springer, Berlin.

Wiggins, S., 1990, *Introduction to Applied Nonlinear Dynamical Systems and Chaos*. Springer, Berlin.

Zaslavsky, G. M., Sagdeev, R. Z., Usikov, D. A. and Chernikov, A. A., 1991. *Weak Chaos and Quasi-Regular Patterns*. Cambridge Nonlinear Science Series, Cambridge.

APPENDIX: CALCULATION OF THE MELNIKOV FUNCTION

The unperturbed manifold

For $\varepsilon = 0$, the flow is steady, so that the trajectories are the curves ψ = constant, with ψ defined as

$$\psi = -\frac{\Gamma}{4\pi}\ln \mathrm{AM}^2 - \frac{\Gamma}{4\pi}\ln \mathrm{BM}^2 = -\frac{\Gamma}{4\pi}\ln(\mathrm{AM}^2\,\mathrm{BM}^2). \tag{A1}$$

It is easy to see that $\mathrm{AM}^2\,\mathrm{BM}^2 = d^4$ = constant on a trajectory. When written using dimensionless variables, this gives $c^4 = d^4/a^4$ = constant with

$$c^4 = [(x-1)^2 + y^2][(x+1)^2 + y^2] = (x^2+y^2)^2 + 2(y^2 - x^2) + 1. \tag{A2}$$

The hyperbolic point $x = y = 0$ belongs to the unperturbed manifold, so that $c = 1$ on the separatrix. It follows that

$$\frac{\mathrm{d}x}{\mathrm{d}t} = -\gamma y(x^2+y^2+1), \qquad \frac{\mathrm{d}y}{\mathrm{d}t} = +\gamma x(x^2+y^2-1) \tag{A3}$$

and

$$(x^2+y^2)^2 = 2(x^2-y^2) \tag{A4}$$

on the manifold. Thus, letting $u = x^2 + y^2$,

$$\frac{\mathrm{d}u}{\mathrm{d}t} = 2\left(x\frac{\mathrm{d}x}{\mathrm{d}t} + y\frac{\mathrm{d}y}{\mathrm{d}t}\right) = -4\gamma xy = -\gamma\sqrt{16x^2y^2} = -\gamma\sqrt{-4(x^2-y^2)^2 + 4(x^2+y^2)^2} \tag{A5}$$

and using eq. (A4)

$$\frac{\mathrm{d}u}{\mathrm{d}t} = -\gamma\sqrt{-(x^2+y^2)^4 + 4(x^2+y^2)^2} = -\gamma\sqrt{-u^4+4u^2} = -\gamma u\sqrt{4-u^2}. \tag{A6}$$

Letting $2v = \sqrt{4-u^2}$, so that $4v^2 = 4 - u^2$ and $8v\,\mathrm{d}v = -2u\,\mathrm{d}u$,

$$\gamma\,\mathrm{d}t = \frac{-\mathrm{d}u}{u\sqrt{4-u^2}} = \frac{-u\,\mathrm{d}u}{u^2\sqrt{4-u^2}} = \frac{4v\,\mathrm{d}v}{(4-4v^2)2v} = \frac{\mathrm{d}v}{2(1-v^2)} = \tfrac{1}{2}\mathrm{d}(\tanh^{-1} v). \tag{A7}$$

At $t = -t_1$, the fluid particle is chosen to lie on the x-axis, so that $y = 0$. Then, according to eq. (A4)

$$0 = x^4 - 2x^2 = x^2(x^2-2) \tag{A8}$$

$x^2(t = -t_1) = 2$ ($x = 0$ represents the hyperbolic fixed point $x = y = 0$) and

$$v(t = -t_1) = \tfrac{1}{2}\sqrt{4 - u^2(t = -t_1)} = \tfrac{1}{2}\sqrt{4-2^2} = 0. \tag{A9}$$

We have $v(t) = \tanh[2\gamma(t+t_1)]$, and

$$x^2 + y^2 = u = 2\sqrt{1-v^2} = 2\sqrt{1-\tanh^2[2\gamma(t+t_1)]} = \frac{2}{\cosh[2\gamma(t+t_1)]}. \tag{A10}$$

Using eq. (A4), we obtain $x^2 - y^2$:

$$x^2 - y^2 = \tfrac{1}{2}(x^2+y^2)^2 = \frac{2}{\cosh^2[2\gamma(t+t_1)]}. \tag{A11}$$

From eqs (A10) and (A11), we derive x^2 and y^2:

$$x^2 = \frac{1}{\cosh[2\gamma(t+t_1)]} + \frac{1}{\cosh^2[2\gamma(t+t_1)]} = 2\frac{\cosh^2[\gamma(t+t_1)]}{\cosh^2[2\gamma(t+t_1)]} \tag{A12}$$

$$y^2 = \frac{1}{\cosh[2\gamma(t+t_1)]} - \frac{1}{\cosh^2[2\gamma(t+t_1)]} = 2\frac{\sinh^2[\gamma(t+t_1)]}{\cosh^2[2\gamma(t+t_1)]}. \tag{A13}$$

Thus,

$$x(t) = \pm\sqrt{2}\frac{\cosh[\gamma(t+t_1)]}{\cosh[2\gamma(t+t_1)]}, \quad y(t) = \pm\sqrt{2}\frac{\sinh[\gamma(t+t_1)]}{\cosh[2\gamma(t+t_1)]} \tag{A14}$$

where the + sign is to be used when $\mathbf{q}_0(0)$ lies on the right unperturbed manifold and the − sign when $\mathbf{q}_0(0)$ is on the left unperturbed manifold.

The Melnikov function

We define the Melnikov function with origin of time at $\mathbf{q}_0(0)$:

$$M_{t_1}(0) = \int_{-\infty}^{+\infty} [f_x[\mathbf{q}_0(t-t_1)]\, g_y[\mathbf{q}_0(t-t_1), t-t_1] - f_y[\mathbf{q}_0(t-t_1)]\, g_x[\mathbf{q}_0(t-t_1), t-t_1]\}\, dt \tag{A15}$$

where $\mathbf{q}_0(t) = [x(t); y(t)]$ on the unperturbed manifold. From eqs (A14), we obtain

$$x[-(t-t_1)] = x[(t-t_1)], \quad y[-(t-t_1)] = -y[(t-t_1)] \tag{A16}$$

on the manifold $\mathbf{q}_0$. Thus, noting that $c = 1$ on the manifold, and letting $x \equiv x(t-t_1)$ and $y \equiv y(t-t_1)$,

$$f_x[\mathbf{q}_0(t-t_1)] = -\gamma y(x^2+y^2+1): \text{ odd function}$$

$$f_y[\mathbf{q}_0(t-t_1)] = +\gamma x(x^2+y^2-1): \text{ even function}$$

$$g_x[\mathbf{q}_0(t-t_1), t-t_1] = -\gamma\, 2xy\cos 2\pi(t-t_1)$$
$$= -\gamma\, 2xy(\cos 2\pi t\cos 2\pi t_1 + \sin 2\pi t\sin 2\pi t_1)$$
$$= (\text{odd fct})\times\cos 2\pi t_1 - (\text{even fct})\times\sin 2\pi t_1$$

$$g_y[\mathbf{q}_0(t-t_1), t-t_1] = +\gamma(x^2-y^2-1)\times\cos 2\pi(t-t_1) = (\text{even fct})\times\cos 2\pi t_1 - (\text{odd fct})\times\sin 2\pi t_1$$

and

$$f_x[\mathbf{q}_0(t-t_1)]\, g_y[\mathbf{q}_0(t-t_1), t-t_1] = (\text{odd fct})\times\cos 2\pi t_1 - (\text{even fct})\times\sin 2\pi t_1$$

$$f_y[\mathbf{q}_0(t-t_1)]\, g_x[\mathbf{q}_0(t-t_1), t-t_1] = (\text{odd fct})\times\cos 2\pi t_1 - (\text{even fct})\times\sin 2\pi t_1.$$

When integrated from $-\infty$ to $+\infty$, which is a symmetrical domain with respect to t, the odd functions disappear, and there remains

$$\begin{aligned} M_{t_1}(0) &= -\sin 2\pi t_1 \times\int_{-\infty}^{+\infty} -\gamma^2\sin 2\pi t[-y(x^2+y^2+1)(x^2-y^2-1) + 2x^2y(x^2+y^2-1)]\, dt \\ &= -\left[\gamma^2\int_{-\infty}^{+\infty} -\sin 2\pi t\, y\{[(y^2+1)^2-x^4] + 2x^2(x^2+y^2-1)\}\, dt\right]\sin 2\pi t_1 \\ &= -\left[\gamma^2\int_{-\infty}^{+\infty} -y\sin 2\pi t[(x^2+y^2+1)^2 - 4x^2]\, dt\right]\sin 2\pi t_1 \end{aligned} \tag{A17}$$

and

$$(x^2+y^2+1)^2 - 4x^2 = (x^2+y^2-2x+1)(x^2+y^2+2x+1) = [(x-1)^2+y^2][(x+1)^2+y^2] = c^4 \tag{A18}$$

with $c = 1$ on the separatrix:

$$M(0) = \gamma^2\left(\int_{-\infty}^{+\infty} y\sin 2\pi t\, dt\right)\sin 2\pi t_1 = \underbrace{\left(\int_{-\infty}^{+\infty} \pm\sqrt{2}\gamma^2\frac{\sinh 2\gamma t}{\cosh 2\gamma t}\sin 2\pi t\, dt\right)}_{F(\gamma)}\sin 2\pi t_1. \tag{A19}$$

According to the table of integrals, series and products (Gradshteyn and Ryzhik, 1980, p. 506), we have:

$$\int_0^\infty \frac{\sin ax\sinh\frac{x}{2}}{\cosh x + \cos\beta}\, dx = \frac{\sinh a\beta}{2\sin\frac{\beta}{2}\cosh a\pi} \tag{A20}$$

with $\beta = \pi/2$:

$$\int_0^\infty \frac{\sin ax\sinh\frac{x}{2}}{\cosh x}\, dx = \frac{\sinh a\frac{\pi}{2}}{\sqrt{2}\cosh a\pi} \tag{A21}$$

$$\begin{aligned} F(\gamma) &= \pm 2\sqrt{2}\gamma^2\int_0^\infty \frac{\sinh 2\gamma t}{\cosh 2\gamma t}\sin 2\pi t\, dt \\ &= \pm\sqrt{2}\gamma\int_0^\infty \frac{\sinh\frac{2\gamma t}{2}}{\cosh 2\gamma t}\sin\frac{\pi}{\gamma}2\gamma t\, d(2\gamma t) \\ &= \pm\sqrt{2}\gamma\int_0^\infty \frac{\sinh\frac{x}{2}}{\cosh x}\sin\frac{\pi}{\gamma}x\, d(x) \end{aligned} \tag{A22}$$

with $a = \frac{\pi}{\gamma}$:

$$F(\gamma) = \pm\gamma\frac{\sinh\frac{\pi^2}{2\gamma}}{\cosh\frac{\pi^2}{\gamma}}. \tag{A23}$$